Applied and Computational Mechanics 6 (2012) 35–52

Applied and Computational Mechanics

Dynamic behavior of Jeffcott rotors with an arbitrary slant crack orientation on the shaft

R. Ramezanpour[a], M. Ghayour[a,*], S. Ziaei-Rad[a]

[a] *Department of Mechanical Engineering, Isfahan University of Technology 84156-83111 Isfahan, Iran*

Received 10 August 2011; received in revised form 10 February 2012

Abstract

Dynamic behaviour of a Jeffcott rotor system with a slant crack under arbitrary crack orientations is investigated. Using concepts of fracture mechanics, flexibility matrix and stiffness matrix of the system are calculated. The system equations motion is obtained in four directions, two transversal, one torsional and one longitudinal, and then solved using numerical method. In this paper a symmetric relation for global stiffness matrix is presented and proved; whereas there are some literatures that reported nonsymmetrical form for this matrix. The influence of crack orientations on the flexibility coefficients and the steady-state response of the system are also investigated. The results indicate that some of the flexibility coefficients are greatly varied by increasing the crack angle from 30° to 90° (transverse crack). It is also shown that some of the flexibility coefficients take their maximum values at (approximately) 60° crack orientation.

Keywords: dynamic, rotor system, slant crack, compliance matrix, response spectrum

1. Introduction

Modern day rotors are designed for achieving higher revolutionary speed. On the other hand such systems have noticeable mass and thus considerable energy. It is obvious that any phenomenon that causes sudden release of this energy may lead to a catastrophic failure in such systems. Since 1980s, numerous researchers have studied the response of rotating systems with crack. Recently [3] investigated a simple Jeffcott rotor with two transverse surface cracks. It is observed significant changes in the dynamic response of the rotor when the angular orientation of one crack relative to the other is varied. A response-dependent nonlinear breathing crack model has been proposed in [2]. Using this model, they studied coupling between longitudinal, lateral and torsional vibrations. They observed that motion coupling together with rotational effect of rotor and nonlinearities due to their presented breathing model introduces sum and difference frequency in the response of the cracked rotor. Transient response of a cracked Jeffcott rotor through passing its critical speed and subharmonic resonance has been analysed by [4]. The peak response variations as well as orbit orientation changes have been also studied experimentally. In comparison to transverse crack, there are a few investigations on slant cracks. A qualitative analysis of a transverse vibration of a rotor system with a crack at an angle of 45 degrees toward the axis of the shaft has been presented in [5]. It has been concluded that the steady-state transversal response of the rotor system contain peaks at the operating speed, twice of the operating speed and their subharmonic frequencies. The transverse vibration of a rotor

*Corresponding author. Tel.: +98 311 3915 247, e-mail: ghayour@cc.iut.ac.ir.

Nomenclature

$A, \bar{A}$	cross sectional area of crack and shaft (m^2)	K_I^i, K_{III}^i	opening and tearing mode of crack due to internal load "i" ($N/m^{3/2}$)
A'	cross sectional area of open part of crack surface (m^2)	$[K]_l$	local stiffness matrix
$[c]_l$	local flexibility matrix of cracked shaft	q_1	longitudinal force (internal reaction) (N)
$[C_s]$	total flexibility matrix of uncracked shaft	q_4, q_5	bending moments (internal reactions) (N · m)
E_{total}	total strain energy of a cracked shaft (N · m)	R_M	radius of the Mohr circle (m)
F_1, F_2, F_{III}	influential functions	T	torsional moment (N · m)
F_x, F_y	transversal forces (external loads) (N)	u	longitudinal displacement of center of disk (m)
F_z	longitudinal force (external load) (N)	U	strain energy of uncracked shaft (N · m)
G	modulus of rigidity (N/m^2)	W	strain energy due to crack (N · m)
h	height of element strip (m)	x, y	transversal displacements of center of disk (m)
$[H]$	transformation matrix	α	rotor center displacement in rotational direction (torsional displacement of center of disk) (rad)
I	moment of inertia for cross section (m^4)	β	rotation angle of element E2 (Mohr circle) (rad)
J	polar moment of inertia of disk (m^2)	γ	crack depth (m)
J_p	polar moment of inertia for cross section (kg · m^2)	η_0	location of elemental strip along η' direction (m)
k_{ij}	cross-coupled stiffness (N/m, N/rad)	θ	crack orientation angle (rad)
k_x, k_y	stiffness in x and y direction (N/m)	σ_M	center of Mohr circle (N/m^2)
k_u	stiffness in longitudinal direction (N/m)	σ_1', σ_2'	axial stress due on element E2 (after rotation) (N/m^2)
k_T	stiffness in torsional direction (N/rad)	τ_1	shear stress on element E1 (before rotation) (N/m^2)
$[k]_g$	global stiffness matrix	τ_1'	shear stress on element E2 (after rotation) (N/m^2)
K_I, K_{III}	total opening and tearing mode of crack ($N/m^{3/2}$)		

system with a slant crack under torsional vibration has been investigated in [6]. It has been considered that the transverse vibration of the rotor is to be closely related to the torsional vibration. A comparison between the response of transverse and slant cracks has been presented in [10]. They proposed use of mechanical impedance for crack detection. It is concluded that vibration behavior of a rotor with a slant crack is less sensitive to mechanical impedance. A simple Jeffcott rotor model of a rotor with a slant crack has been considered by [1]. It is observed a rotor with a slant crack is stiffer in lateral and longitudinal directions, but more flexible in torsion, compared to a rotor with a transverse crack. Recently [8] in his good review paper explained many crack models such as open crack model, switching crack model, second moment inertia model, breathing models and harmonic model approaches. The dynamics behaviour of a slant (45° crack angle) cracked rotor has been studied by [7]. Using Jeffcott rotor model, the equation of the motion extracted in four directions. Global stiffness of the system obtained from concepts of fracture mechanics and strain energy release rate. It is included that existence of the frequency of torsional excitation in longitudinal response and combined frequencies of the rotating frequency and frequency of torsional excitation in transversal response are good signs for slant crack detection.

In this paper, the dynamic behavior of a cracked Jeffcott rotor with a slant crack on the shaft is considered. Motion equations of the system that are obtained in four directions, two transver-

sal, one torsional and one longitudinal, are solved by Runge-Kutta method. Using concepts of fracture mechanics, flexibility matrix and thus stiffness matrix of the system are calculated. Also the influence of crack orientations on the flexibility coefficients and subsequently on the amplitude of the frequency responses in several prominent frequencies is investigated. These results depict a better understanding for the dynamic behavior of slant cracked shaft under various crack orientations.

2. Equations of motion

Consider a Jeffcott rotor rotating at speed Ω (Fig. 1). The shaft is assumed to be massless and a disk of mass m is placed in the middle of the shaft. A view of cross section of the disk is shown in Fig. 2. In this figure XOY is the fixed coordinate, $\xi o\eta$ is the rotational coordinate with center o and $\xi' o'\eta'$ is rotational coordinate that is located at the center of the disk and attached to it. Point o' is the center of the disk, c is the disk center of mass, α is the angle represents the torsional vibration of the system and φ is the angle between center of mass and rotational coordinate.

In the following equations indices u and T denote the coefficient for torsional and longitudinal directions respectively. Using d'Alambert principle (Fig. 3), equation of the motion in four directions (two transversal, one torsional and one longitudinal) can be established as

$$\begin{aligned} &m\ddot{x} + c\dot{x} + k_x x + k_{xy} y + k_{xT}\alpha + k_{xu} u = \\ &-mg + me(\Omega + \dot{\alpha})^2 \cos(\Omega t + \alpha + \varphi) + me\ddot{\alpha} \sin(\Omega t + \alpha + \varphi), \end{aligned} \tag{1}$$

$$\begin{aligned} &m\ddot{y} + c\dot{y} + k_{xy} x + k_y y + k_{yT}\alpha + k_{yu} u = \\ &me(\Omega + \dot{\alpha})^2 \sin(\Omega t + \alpha + \varphi) - me\ddot{\alpha} \cos(\Omega t + \alpha + \varphi), \end{aligned} \tag{2}$$

$$\begin{aligned} &J\ddot{\alpha} + c_T(\Omega + \dot{\alpha}) + k_{xT} x + k_{yT} y + k_T \alpha + k_{Tu} u = \\ &M(t) + mge \sin(\Omega t + \alpha + \varphi) + me\ddot{x} \sin(\Omega t + \alpha + \varphi) - m\ddot{y} e \cos(\Omega t + \alpha + \varphi), \end{aligned} \tag{3}$$

$$m\ddot{u} + c_u \dot{u} + k_{xu} x + k_{yu} y + k_{Tu}\alpha + k_u u = 0, \tag{4}$$

where J is the mass moment of inertia of the disk about o', c, c_T, and c_u are the damping coefficients in transversal, torsional and longitudinal directions. It should be mentioned that these equations are the same with those reported in [7]. Also, $M(t)$ is the torsional excitation and e is the eccentricity of the disk. According to (1)–(4) the stiffness matrix of the system can be extracted as:

$$F = \begin{bmatrix} k_x & k_{xy} & k_{xT} & k_{xu} \\ k_{xy} & k_y & k_{yT} & k_{yu} \\ k_{xT} & k_{yT} & k_T & k_{Tu} \\ k_{xu} & k_{yu} & k_{Tu} & k_u \end{bmatrix} \begin{pmatrix} x \\ y \\ \alpha \\ u \end{pmatrix} \Rightarrow [k]_g = \begin{bmatrix} k_x & k_{xy} & k_{xT} & k_{xu} \\ k_{xy} & k_y & k_{yT} & k_{yu} \\ k_{xT} & k_{yT} & k_T & k_{Tu} \\ k_{xu} & k_{yu} & k_{Tu} & k_u \end{bmatrix}. \tag{5}$$

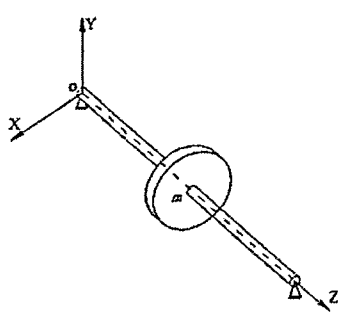

Fig. 1. A schematic of Jeffcott rotor

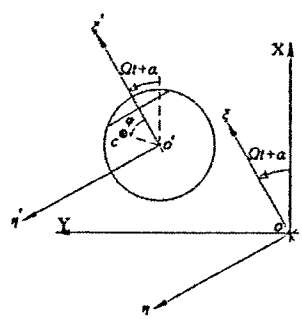

Fig. 2. Cross sectional view of crack at middle point of the shaft

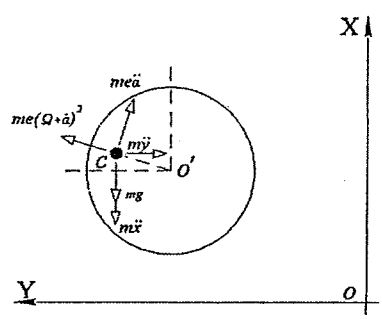

Fig. 3. Forces exerted on the mass center of the disk

Existence of crack can affect the elements of this matrix. This will be shown in the following sections.

3. Flexibility of a rotor with slant crack

In this section using strain energy release rate method and Castigliano's theorem, the crack compliance matrix is calculated. It is known that the total strain energy of a cracked shaft is the sum of strain energy of uncracked shaft and strain energy caused by crack.

$$E_{\text{total}} = U_{\text{uncracked shaft}} + W_{\text{cracked shaft}}. \tag{6}$$

Consider a cracked shaft (Fig. 4) under four external loads, three forces exerted in principle directions and one torsional moment in Z directions. Thus, the strain energy of an uncracked shaft can be expressed as

$$U = \frac{F_x^2 l^3}{96EI} + \frac{F_y^2 l^3}{96EI} + \frac{T^2 l}{4GJ_p} + \frac{F_z^2 l}{4\bar{A}E}, \tag{7}$$

where G is the shear modulus and $\bar{A}$ is the cross sectional area of the shaft.

Suppose that internal reactions on an element of shaft containing crack, are two bending moments q_4 and q_5, one torsional moment T and one longitudinal force q_1 (Fig. 5). Thus the additional strain energy due to crack is a function of q_5, q_4, T and q_1.

According to (6) and also using Castigliano's theorem, the local flexibility of cracked shaft will be determine using following relation

$$\frac{\partial^2 E}{\partial F_i \partial F_j} = \frac{\partial^2 U}{\partial F_i \partial F_j} + \frac{\partial^2 W}{\partial F_i \partial F_j}. \tag{8}$$

If there is not exist a crack on the shaft, the flexibility due to crack is zero. Therefore, flexibility of the system will be equal to the flexibility of an uncracked shaft. Using (7), the first term in the right hand side of (8) can be determined.

The next step is to find relations between F_i and q_i. Using Figs. 6a and 6b, the following relations can be obtained

$$q_4 = \frac{F_y}{2}\left(\frac{l}{2}\right) = \frac{F_y l}{4}, \qquad q_5 = \frac{F_x}{2}\left(\frac{l}{2}\right) = \frac{F_x l}{4}. \tag{9}$$

Considering (9) and using the chain rule, (8) leads to flexibility matrix of cracked shaft, $[c]_l$ (see

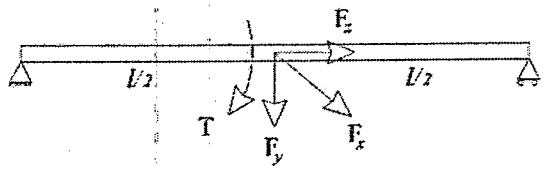

Fig. 4. A cracked shaft under external loads

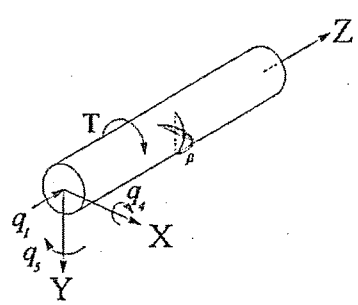

Fig. 5. Internal reactions on the crack

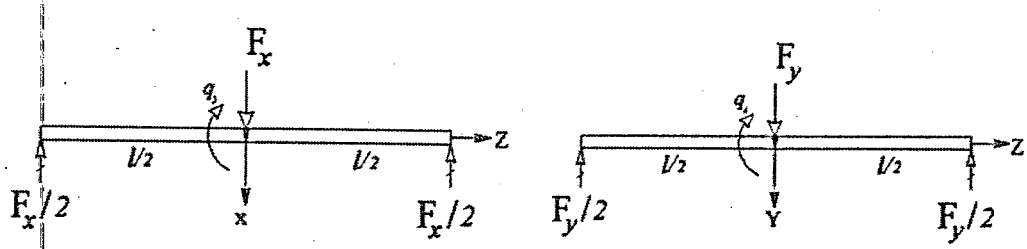

(a) (b)

Fig. 6. Relation between external and internal loads: (a) between F_x and q_5, (b) between F_y and q_4

Appendix I)

$$[c]_l = \begin{bmatrix} \frac{l^2}{16}\left(\frac{\partial^2 W}{\partial q_5^2}\right) & \frac{l^2}{16}\left(\frac{\partial^2 W}{\partial q_5 \partial q_4}\right) & \frac{l}{4}\left(\frac{\partial^2 W}{\partial q_5 \partial T}\right) & \frac{l}{4}\left(\frac{\partial^2 W}{\partial q_5 \partial q_1}\right) \\ & \frac{l^2}{16}\left(\frac{\partial^2 W}{\partial q_4^2}\right) & \frac{l}{4}\left(\frac{\partial^2 W}{\partial q_4 \partial T}\right) & \frac{l}{4}\left(\frac{\partial^2 W}{\partial q_4 \partial q_1}\right) \\ & & \frac{\partial^2 W}{\partial T^2} & \frac{\partial^2 W}{\partial q_1 \partial T} \\ \text{sym.} & & & \frac{\partial^2 W}{\partial q_1^2} \end{bmatrix} + \text{diag}\left(\frac{l^3}{48EI}, \frac{l^3}{48EI}, \frac{l}{2GJ_p}, \frac{l}{2AE}\right). \tag{10}$$

Eq. (10) can be written in compact form as

$$[c]_l = [G_1][\Delta c_{ij}][G_2] + [C_s], \tag{11}$$

where

$$\Delta c_{ij} = \frac{\partial^2 W}{\partial q_i \partial q_j}, \quad [G_1] = \left[\frac{l}{4}, \frac{l}{4}, 1, 1\right], \quad [G_2] = \left[\frac{l}{4}, \frac{l}{4}, 1, 1\right], \quad [C_s] = \text{diag}\left(\frac{l^3}{48EI}, \frac{l^3}{48EI}, \frac{l}{2GJ_p}, \frac{l}{2AE}\right). \tag{12}$$

It is obvious that (11) leads to a symmetric matrix whereas some researchers reported non symmetric form for it [8,9]. Using to (11), one is able to determine local flexibility of a cracked shaft if additional strain energy due to crack can be determined. This is feasible using concepts of fracture mechanics. According to [7], strain energy due to crack is given by

$$W = \int_{A'} \frac{1}{E'} K_I^2 \, \mathrm{d}A' + \int_A \frac{1}{E'}(1+\nu) K_{III}^2 \, \mathrm{d}A, \tag{13}$$

where for tearing mode (K_{III}) the total surface of crack, i.e. A, is used for integration while for the opening mode (K_I) part of the crack surface which remains open during the rotation, A', should be taking into account [7].

Crack surface at θ orientation is shown in Fig. 7. Using this figure (Fig. 7) the stress intensity factors for a slant crack at θ angle are given by

For q_1,

$$K_I^1 = \frac{q_1}{\pi R^2} \sin^2(\theta) \sqrt{\pi\gamma} F_1, \quad K_{III}^1 = \frac{q_1}{\pi R^2} \sin(\theta \cos(\theta) \sqrt{\pi\gamma} F_{III}. \tag{14}$$

For q_4,

$$K_I^4 = \frac{4q_4 x_0}{\pi R^4} \sin^2(\theta) \sqrt{\pi\gamma} F_1, \quad K_{III}^4 = \frac{2q_4 x_0}{\pi R^4} \sin(\theta) \cos(\theta) \sqrt{\pi\gamma} F_{III}. \tag{15}$$

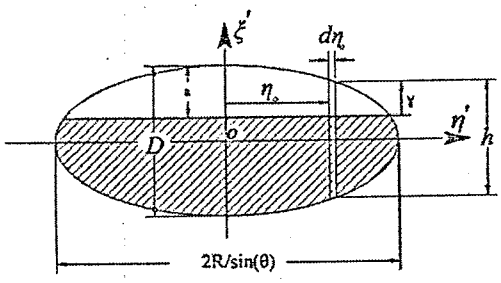

Fig. 7. The crack surface at orientation angle θ

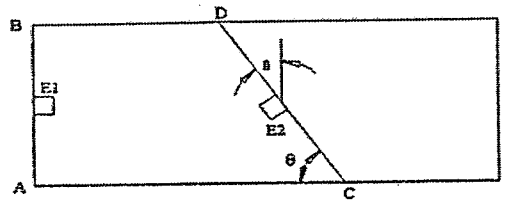

Fig. 8. The location of elements E1 and E2 used in Mohr circle

For q_5,

$$K_I^5 = \frac{4q_5\sqrt{R^2-x_0^2}}{\pi R^4}\sin^2(\theta)\sqrt{\pi\gamma}F_2, \quad K_{III}^5 = \frac{2q_5}{\pi R^4}\sin(2\theta)\sqrt{\pi\gamma}F_{III}. \tag{16}$$

And finally for T,

$$K_I^T = \frac{2T\sqrt{R^2-x_0^2}}{\pi R^4}\sin(2\theta)\sqrt{\pi\gamma}F_2, \tag{17}$$

$$K_{III}^T = \frac{-2T\sqrt{R^2-x_0^2}}{\pi R^4}\cos(2\theta)\sqrt{\pi\gamma}F_{III}, \tag{18}$$

where

$$x_0 = \eta_0\sin(\theta). \tag{19}$$

According to [11]

$$F_1 = \sqrt{\frac{\tan(\lambda)}{\lambda}}\left[0.752 + 1.01\frac{\gamma}{\sqrt{R^2-x_o^2}} + 0.37(1-\sin(\lambda))^3\right]\frac{1}{\cos(\lambda)}, \tag{20a}$$

$$F_2 = \sqrt{\frac{\tan(\lambda)}{\lambda}}\left[0.923 + 0.199(1-\sin(\lambda))^4\right]\frac{1}{\cos(\lambda)}, \tag{20b}$$

$$F_{III} = \sqrt{\frac{\tan(\lambda)}{\lambda}}, \quad \lambda = \frac{\pi\gamma}{4\sqrt{R^2-x_o^2}}. \tag{20c}$$

Therefore, the total strain density functions are

$$K_I = \left(\frac{q_1}{\pi R^2}\sin^2(\theta)F_1 + \frac{4q_4x_0}{\pi R^4}\sin^2(\theta)F_1 + \frac{4q_5\sqrt{R^2-x_0^2}}{\pi R^4}\sin^2(\theta)F_2 + \frac{2T\sqrt{R^2-x_0^2}}{\pi R^4}\sin(2\theta)F_2\right)\sqrt{\pi\gamma}, \tag{21}$$

$$K_{III} = \left(\frac{q_1}{\pi R^2}\sin(\theta)\cos(\theta) + \frac{2q_5}{\pi R^4}\sin(2\theta) - \frac{2T\sqrt{R^2-x_0^2}}{\pi R^4}\cos(2\theta)\right)\sqrt{\pi\gamma}F_{III}. \tag{22}$$

Eq. (18) has appeared in different forms in literature [1, 2]. Here, we have used Mohr circle to extract its correct form. To show this, let consider two elements E1 and E2 as depicted in Fig. 8. Element E1 coincides with element E2 after rotating it β degree counterclockwise where

$$\beta = \frac{\pi}{2} - \theta. \tag{23}$$

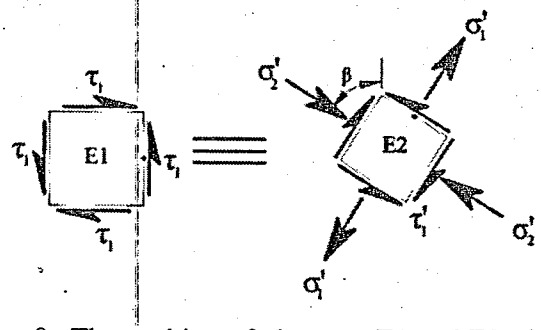

Fig. 9. The position of elements E1 and E2 after rotation β (CCW)

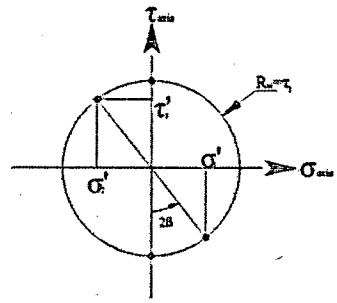

Fig. 10. The Mohr circle (center σ_M and radius R_M)

It is obvious that in relation (18), the stress intensity factor is due to the torsional moment T. Torsional moment T creates shear stress τ_1 equal to

$$\tau_1 = \frac{T\sqrt{R^2 - x_0^2}}{(\pi R^4/2)}. \tag{24}$$

Shear stress τ_1 on element E1 and stresses on element E2 are shown in Fig. 9.

From equalizing these to configurations, the center σ_M and radius R_M of the Mohr circle are zero and τ_1 respectively so according to Fig. 10, one can obtain

$$\sigma_1' = \tau_1 \sin(2\beta) = \tau_1 \sin(\pi - 2\theta) = \tau_1 \sin(2\theta), \tag{25}$$

$$\sigma_2' = -\tau_1 \sin(2\theta), \tag{26}$$

$$\tau_1' = \tau_1 \cos(2\beta) = -\tau_1 \cos(2\theta). \tag{27}$$

Thus, the correct form of the stress intensity factor for the third mode caused by T is given by

$$K_{III}^T = \frac{2T\sqrt{R^2 - x_0^2}}{\pi R^4} \cos(2\beta)\sqrt{\pi\gamma} F_{III} = \frac{-2T\sqrt{R^2 - x_0^2}}{\pi R^4} \cos(2\theta)\sqrt{\pi\gamma} F_{III}. \tag{28}$$

After calculating the local flexibility of a cracked rotor, local stiffness of the system can be calculated

$$[K]_l = [c]_l^{-1}. \tag{29}$$

The global stiffness matrix in the inertia coordinate system is

$$[K]_g = [H]^{-1}[K]_l[H], \tag{30}$$

where

$$[H] = \begin{bmatrix} \cos(\Phi) & \sin(\Phi) & 0 & 0 \\ -\sin(\Phi) & \cos(\Phi) & 0 & 0 \\ 0 & 0 & 1 & 0 \\ 0 & 0 & 0 & 1 \end{bmatrix}, \quad \Phi = \Omega t + \alpha. \tag{31}$$

For a 9.5 mm diameter shaft with a crack depth equal to its radius, the elements of the local flexibility matrix are evaluated for different crack orientations from 30° to 90° (transverse crack). In Fig. 11 the variations of these flexibilities versus CCLP[1] [2] and crack orientations (30°, 45°, 60°, 70°, 80° and 90°) are shown. It should be mentioned that the crack tip is divided into

[1] Crack closure line position

360 point for using CCLP method. It means that for CCLP = 180 the crack is fully open and CCLP = 0 or 360 exhibits a fully closed crack.

According to Fig. 11, increasing the value of crack angle increases the maximum value of $c(1,1)$ and $c(2,2)$. In fact the maximum value of these coefficients occurs when the crack is fully open (i.e. CCLP = 180). When the crack is fully open, in bending, the flexibility of the transverse crack is more than that of the slant crack and flexibility is a monotonic function of the crack angle. For fully open crack $c(3,3)$ for slant crack is higher than the transverse one. When the crack is fully closed, the value of $c(1,1)$ for slant crack is higher than the transverse one. However, there is no difference between the values of $c(2,2)$ for slant crack and transverse crack (for fully closed crack).

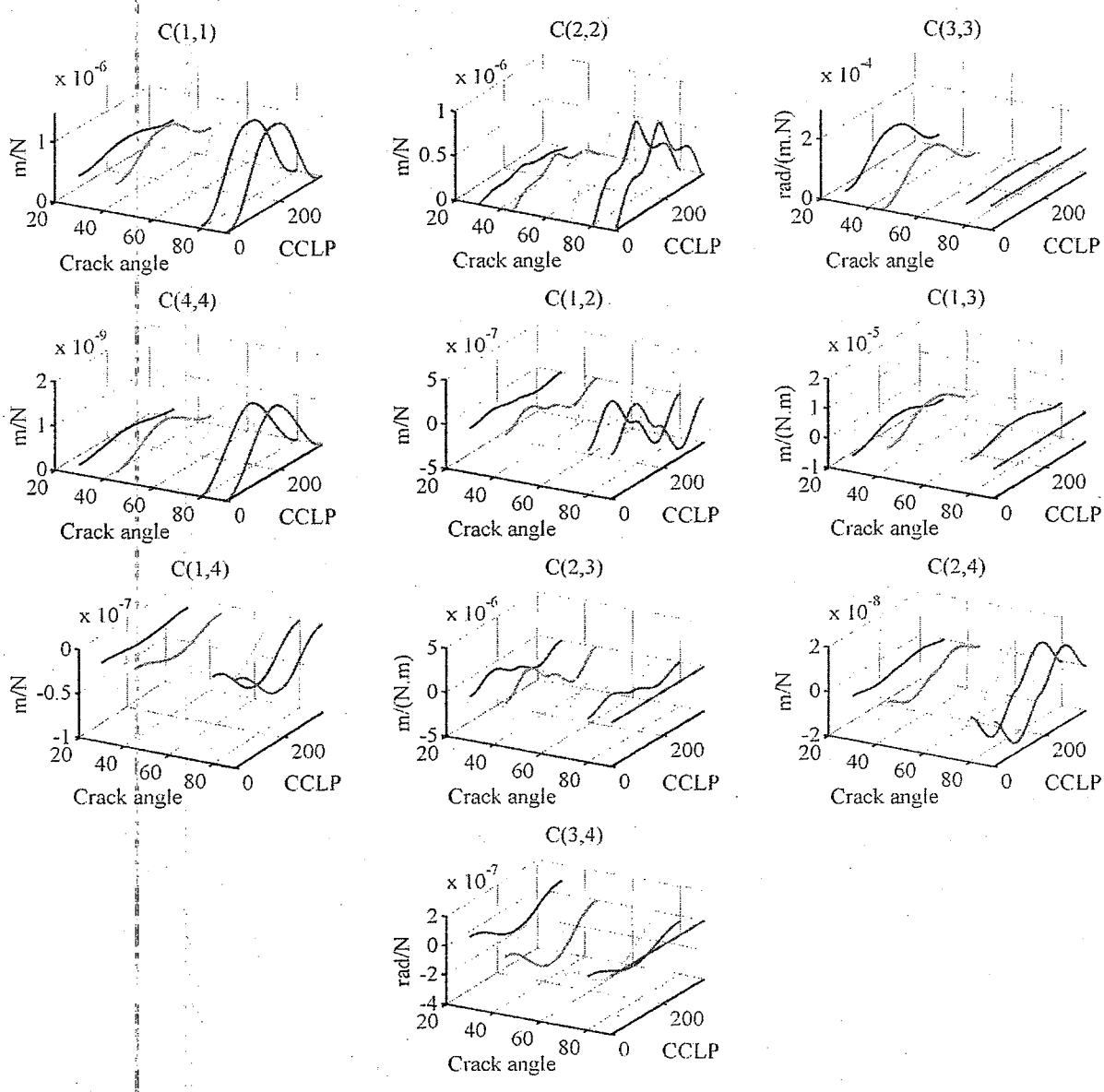

Fig. 11. Variation of the elements of local flexibility matrix versus CCLP and crack orientation from 30° to 90°

Fig. 11 shows that generally in torsion, slant crack is more critical than the transverse crack. Similar conclusion is presented in [1]. Whereas for closed crack, transverse one is flexible than slant one. It should be mentioned that for a fully closed crack, the slant crack with 45° orientation angle has no corresponding flexibility coefficient in torsion. This is due to the fact

that according to relation (22), when θ is $\pi/2$, stress intensity factor in 3rd mode that caused by T will be zero. Therefore, among slant cracks with different orientations, 45° slant crack has the minimum value in torsion.

It should be noticed that $c(3,3)$ coefficient for a transverse crack is not sensitive to the amount of the open part of crack. In other words the value of $c(3,3)$ does not depend on the value of CCLP. $c(1,2)$ and $c(2,4)$ in CCLP = 0, CCLP = 180 and CCLP = 360 are zero, but in other CCLPs are not zero.

The elements of $c(2,4)$ and $c(1,2)$ for open and closed cracks are not depended on the crack angle. In other words, $c(2,4)$ and $c(1,2)$ do not have any rule in coupling between the bending in different directions. If one considers the breathiong crack, the elements obtain their maximum at CCLP = 90 and 270. Elements $c(4,4)$ and $c(1,4)$ have a trend similar to $c(1,1)$. For fully closed crack the value of $c(4,4)$ and $c(1,4)$ for slant crack are higher than the transverse one.

From Fig. 11 it can be seen that the coefficients $c(1,3)$ and $c(2,3)$ are zero for transverse crack. These elemnts cause coupling between torsional and transversal directions. This means that the effects of coupling for slant crack is more than the transverse one. Therefore, in general it is resonable that one expects there exist more frequencies in the spectrums of responses for the slant crack in comparison to those relate to the transverse one.

It is worth mentioning that from Fig. 11, one can observe that the maximum value of elements $c(1,3)$, $c(2,3)$ and $c(3,4)$ versus crack angle occurs at 60 degrees for open crack. However, for open crack $c(2,3)$ does not have any rule in coupling between torsional and bending vibration.

4. Vibration response of rotor system with slant crack

The parameters that are needed for solving (1)–(4) are tabulated here (Table 1).

Table 1. Solution parameters

Revolutionary speed	$\Omega = 500$ rpm	Disk mass	$m = 0.595$ kg
Torsional excitation freq.	$\omega_T = 0.6\Omega = 300$ rpm	Shaft length	$l = 0.26$ m
External torsional excitation	$M(t) = \sin(\omega_T t)$	Shaft diameter	$D = 9.5$ mm
Transversal damp coefficient	$c = 41.65$ kg/s	Disk diameter	$dp = 76$ mm
Torsional damp coefficient	$c_T = 0.009\,1$ kg $\cdot$ m^2/s	Initial phase angle	$\varphi = \pi/6$ rad
Longitudinal damp coefficient	$c_u = 146.203\,4$ kg/s	Poisson ratio	$\nu = 0.3$
Modulus of elasticity	$E = 210$ GPa	Eccentricity	$e = 0.164\,3$ mm

Solution of motion equations considering breathing model for the crack is very time consuming in comparison to open crack model. On the other hand, there are the same prominent characteristic frequencies for these two models [7]. Therefore, all calculations in this paper are about open crack model and its effects on the response of the system. Runge-Kutta method is used for solving the equations of the motion. Using this method, the response of the Jeffcott rotor with a slant crack under different crack angles is evaluated. Figs. 12–15 show the system responses for crack orientations 30°, 45°, 60° and 90° respectively. Theses responses are related to two transversal, one torsional and one longitudinal direction. It should be mentioned that response for other angles such as 60°, 70° and 80° are obtained but are not presented here.

According to Fig. 12, for 30° slant crack, the spectrum of transversal (vertical and horizontal) responses contain Ω and 2Ω frequencies and their side bands ($\Omega \pm \omega_T$ and $2\Omega \pm \omega_T$). Fig. 13 show that there are Ω, 2Ω, $\Omega \pm \omega_T$, $2\Omega \pm \omega_T$ and 3Ω frequencies in the spectrum of

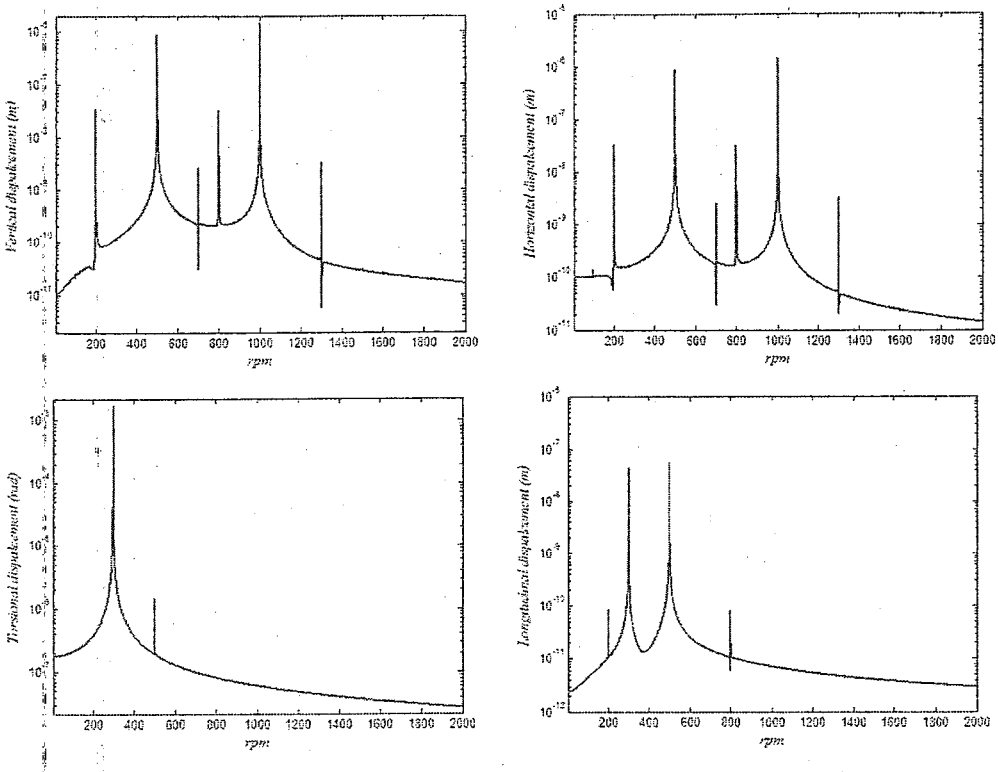

Fig. 12. Spectrum of the rotor response for 30° slant crack

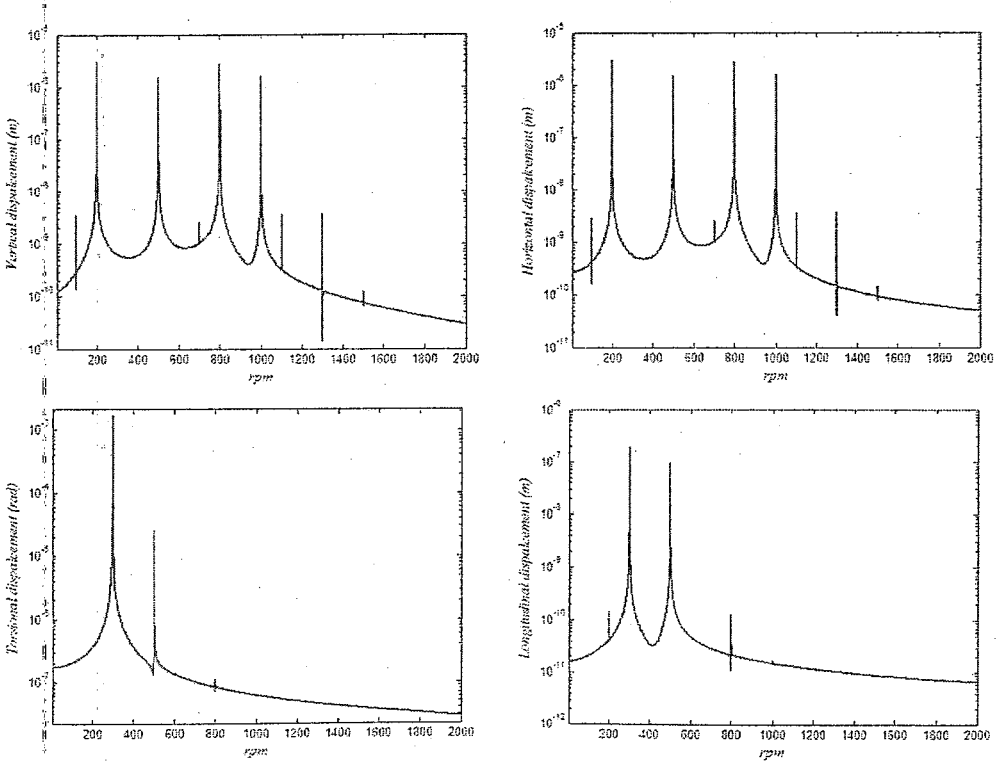

Fig. 13. Spectrum of the rotor response for 45° slant crack

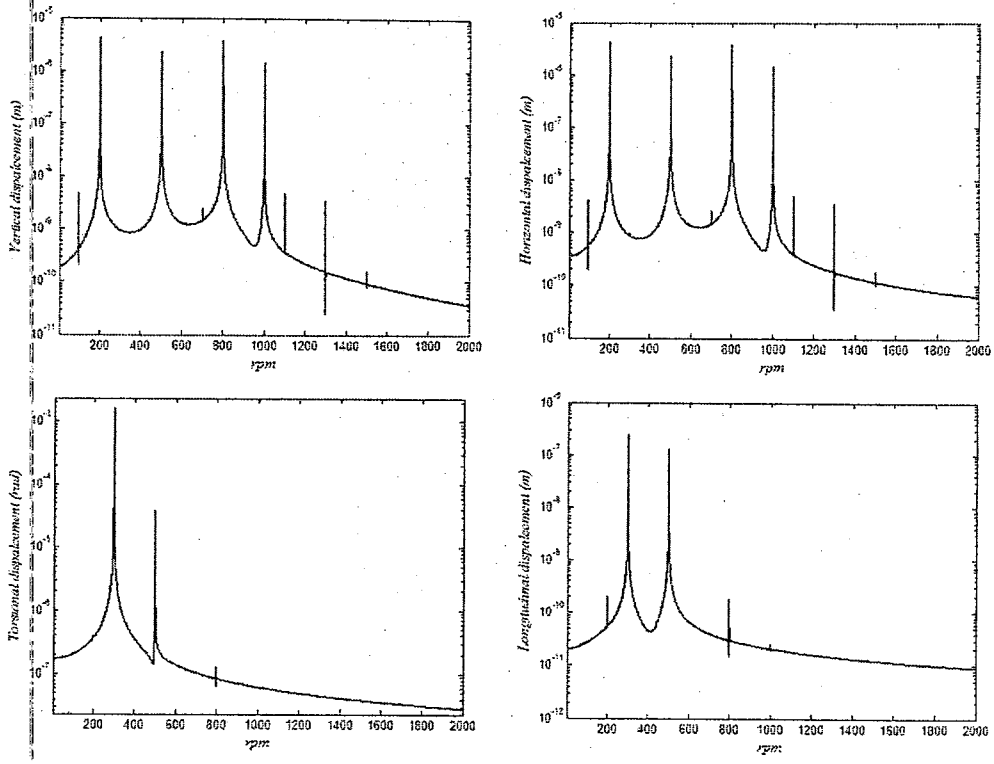

Fig. 14. Spectrum of the response for 60° slant crack

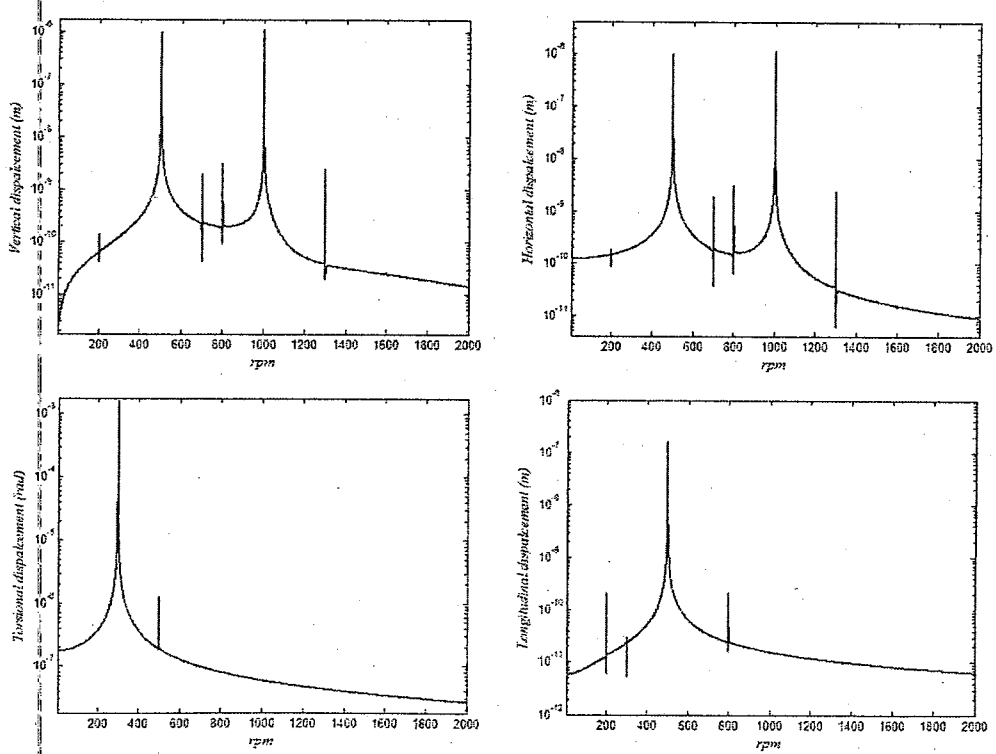

Fig. 15. Spectrum of the response for 90° slant crack

transversal responses for 45° slant cracks. Whereas there is only Ω, 2Ω, $\Omega \pm \omega_T$ and $2\Omega \pm \omega_T$ frequencies in the spectrum of transversal response for transverse crack. It is considerable that general schemas of spectrums of 30° and 90° slant cracks are almost the same and have sensible difference in compare to other spectrums. It can be explained that there are three coefficients ($c(1,3)$, $c(2,3)$ and $c(3,4)$) in the flexibility matrix that can cause coupling between torsional and other directions. Among these coefficients, there are two coefficients that can cause coupling between transversal and torsional response and they are $c(1,3)$ and $c(3,4)$. On the other hand for fully open crack $c(2,3)$ is zero.

According to Fig. 11, it can be seen that $c(1,3)$, for 30° slant crack and 90° slant crack are equal to each other and both of them are zero; therefor spectrums of transversal responses for both of them (30° and 90° slant crack) have the same schema. It should be noticed that existence of combined frequencies such as $\Omega \pm \omega_T$ and $2\Omega \pm \omega_T$ in the spectrum of transversal response (for 30° and 90°) are due to coupling phenomena that caused by eccentricity (that can be seen in the equations of the motion).

The spectrums of torsional responses (Figs. 12–15) for all crack angles contain Ω and ω_T frequencies. Also all the mentioned spectrums have $\Omega + \omega_T$ frequency except in spectrums with 30° and 90° slant cracks. Existence of Ω, ω_T and $\Omega \pm \omega_T$ frequencies in the spectrums of longitudinal responses (Figs. 12–15) is obvious. In all of these spectrums, the 2Ω frequency can be detected. However, as the peaks are very small in 30° and 90° slant crack, they are not easily detectable. It is clear that the amplitude of frequency response functions for different crack angles are not equal.

Fig. 16 compares these amplitudes at the prominent frequencies (Ω, 2Ω, $\Omega \pm \omega_T$ and $2\Omega \pm \omega_T$ for transversal, Ω and ω_T for torsional and longitudinal spectrums [7]).

According to Fig. 16, in Ω frequency, when the crack angle increases from 30° to 60°, the amplitude of transversal responses increase to maximum, then increasing in the crack angle from 80° to 90° increases the amplitude. In 2Ω frequency, increasing in the crack angle from 30° to 45°, increases the value of amplitude of the transversal responses and then from 45° to 90° the mentioned amplitude decreases. The $\Omega \pm \omega_T$ frequencies in the transversal responses have the same variations versus crack angles. In these frequencies, any increase in the crack orientations from 30° to 60°, increases the amplitude of transversal responses and any increase in the crack angle from 60° to 90° decreases the amplitude of them. In Ω frequency the amplitude of torsional responses increases when the crack angle increases from 30° to 60°. Whereas from 60° to 90°, any increase in the crack angle, decreases the amplitude. In these spectrums and for ω_T frequency, any increase from 30° to 90° increases amplitude. In Ω frequency, any increase in the crack angle from 30° to 90°, increases the amplitude of longitudinal responses. However in these spectrums and for ω_T frequency, any increase in crack angle from 30° to 60°, increases the amplitude of these responses and for crack angles between 60° to 90° decreases them.

5. Conclusions

In this paper the dynamic behavior of a Jeffcott rotor system with a slant crack under arbitrary crack orientations is investigated. Using concepts of fracture mechanics, flexibility matrix and subsequently stiffness matrix of the system are evaluated and the influence of crack orientations on the flexibility coefficients is investigated. In this paper a symmetric relation for global stiffness matrix is presented and proved; whereas there are some literatures that reported non-symmetrical form for this matrix. It is shown that for fully open crack $c(1,1)$, $c(2,2)$, $c(4,4)$, and $c(1,4)$ coefficients are more for transverse crack rather than slant crack. For slant crack,

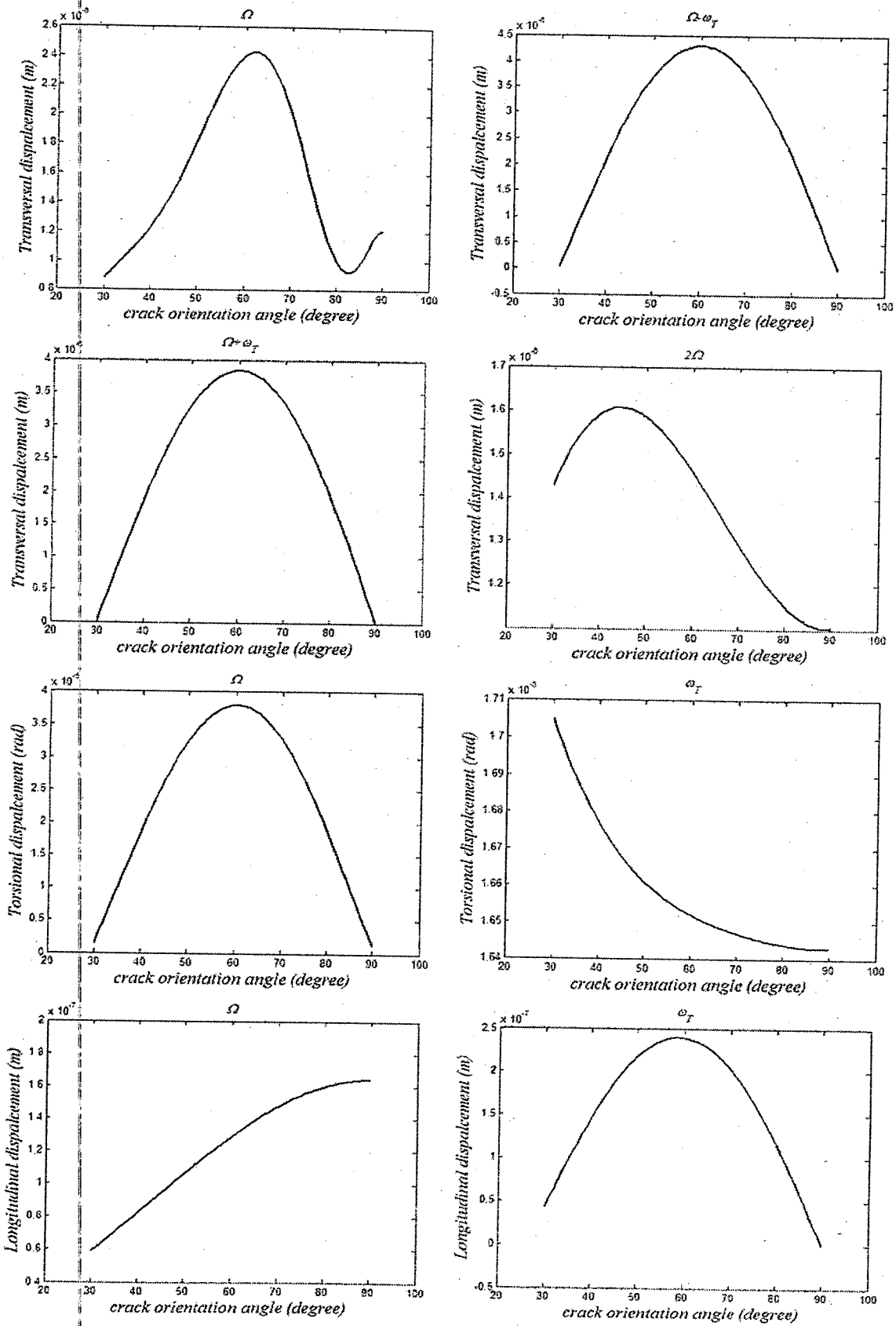

Fig. 16. Variation of flexibility coefficients with crack orientation angle

the more crack angle is, the more $c(3,3)$ coefficient will be. However for 60° slant crack $c(3,4)$ and $c(1,3)$ will be max and it shows that for 60° slant crack, the stiffness coupling between torsional direction and other directions increases. Therefor in the transversal response and in $\Omega \pm \omega_T$ frequencies, there is a maximum in the amplitude of the spectrum for 60° slant crack. In similar, there is a maximum in the amplitude of longitudinal response at 60° crack angle, because there is a maximum for $c(3,4)$ coefficient in this angle.

Also It is shown that the amplitude of transversal response in the Ω, $\Omega \pm \omega_T$, and 2Ω frequencies will be maximum at 60°, 60° and 45° crack angles respectively. For 60° slant crack, the amplitude of torsional response in Ω frequency and the amplitude of longitudinal response in ω_T frequency are maximum.

Appendix A

Considering (9) and using chain rule we have

$$\begin{aligned}
\frac{\partial^2 W}{\partial F_x^2} &= \frac{\partial}{\partial F_x}\left(\frac{\partial W}{\partial q_5}\cdot\frac{\partial q_5}{\partial F_x}\right) = \frac{\partial^2 W}{\partial q_5^2}\cdot\left(\frac{\partial q_5}{\partial F_x}\right)^2 + \frac{\partial W}{\partial q_5}\cdot\frac{\partial^2 q_5}{\partial F_x^2} = \\
&\quad \frac{\partial^2 W}{\partial q_5^2}\cdot\left(\frac{l}{4}\right)^2 = \frac{l^2}{16}\left(\frac{\partial^2 W}{\partial q_5^2}\right), \\
\frac{\partial^2 W}{\partial F_y^2} &= \frac{\partial}{\partial F_y}\left(\frac{\partial W}{\partial q_4}\cdot\frac{\partial q_4}{\partial F_y}\right) = \frac{\partial^2 W}{\partial q_4^2}\cdot\left(\frac{\partial q_4}{\partial F_y}\right)^2 + \frac{\partial W}{\partial q_4}\cdot\frac{\partial^2 q_4}{\partial F_y^2} = \frac{l^2}{16}\left(\frac{\partial^2 W}{\partial q_4^2}\right), \\
\frac{\partial^2 W}{\partial F_z^2} &= \frac{\partial}{\partial F_z}\left(\frac{\partial W}{\partial q_1}\cdot\frac{\partial q_1}{\partial F_z}\right) = \frac{\partial^2 W}{\partial q_1^2}\cdot\left(\frac{\partial q_1}{\partial F_z}\right)^2 + \frac{\partial W}{\partial q_1}\cdot\frac{\partial^2 q_1}{\partial F_z^2} = \frac{\partial^2 W}{\partial q_1^2}, \\
\frac{\partial^2 W}{\partial T^2} &= \frac{\partial^2 W}{\partial T^2}
\end{aligned} \tag{A–1}$$

and

$$\begin{aligned}
\frac{\partial^2 W}{\partial F_x \partial F_y} &= \frac{\partial}{\partial F_x}\left(\frac{\partial W}{\partial q_4}\cdot\frac{\partial q_4}{\partial F_y}\right) = \frac{\partial^2 W}{\partial q_5 \partial q_4}\cdot\frac{\partial q_5}{\partial F_x}\cdot\frac{\partial q_4}{\partial F_y} + \frac{\partial W}{\partial q_4}\cdot\frac{\partial^2 q_4}{\partial F_x \partial F_y} = \\
&\quad \left(\frac{l}{4}\right)\left(\frac{l}{4}\right)\left(\frac{\partial^2 W}{\partial q_5 \partial q_4}\right) = \frac{l^2}{16}\left(\frac{\partial^2 W}{\partial q_5 \partial q_4}\right), \\
\frac{\partial^2 W}{\partial F_x \partial F_z} &= \frac{\partial}{\partial F_x}\left(\frac{\partial W}{\partial q_1}\cdot\frac{\partial q_1}{\partial F_z}\right) = \frac{\partial^2 W}{\partial q_5 \partial q_1}\cdot\frac{\partial q_5}{\partial F_x}\cdot\frac{\partial q_1}{\partial F_z} + \frac{\partial W}{\partial q_1}\cdot\frac{\partial^2 q_1}{\partial F_x \partial F_z} = \frac{l}{4}\left(\frac{\partial^2 W}{\partial q_5 \partial q_1}\right), \\
\frac{\partial^2 W}{\partial F_x \partial T} &= \frac{\partial}{\partial F_x}\left(\frac{\partial W}{\partial T}\right) = \frac{\partial^2 W}{\partial q_5 \partial T}\cdot\frac{\partial q_5}{\partial F_x} = \frac{l}{4}\left(\frac{\partial^2 W}{\partial q_5 \partial T}\right), \\
\frac{\partial^2 W}{\partial F_y \partial F_z} &= \frac{\partial}{\partial F_y}\left(\frac{\partial W}{\partial q_1}\cdot\frac{\partial q_1}{\partial F_z}\right) = \frac{\partial^2 W}{\partial q_4 \partial q_1}\cdot\frac{\partial q_4}{\partial F_y}\cdot\frac{\partial q_1}{\partial F_z} + \frac{\partial W}{\partial q_1}\cdot\frac{\partial^2 q_1}{\partial F_y \partial F_z} = \frac{l}{4}\left(\frac{\partial^2 W}{\partial q_4 \partial q_1}\right), \\
\frac{\partial^2 W}{\partial F_y \partial T} &= \frac{\partial}{\partial F_y}\left(\frac{\partial W}{\partial T}\right) = \frac{\partial^2 W}{\partial q_4 \partial T}\cdot\frac{\partial q_4}{\partial F_y} = \frac{l}{4}\left(\frac{\partial^2 W}{\partial q_4 \partial T}\right), \\
\frac{\partial^2 W}{\partial F_z \partial T} &= \frac{\partial}{\partial F_z}\left(\frac{\partial W}{\partial T}\right) = \frac{\partial^2 W}{\partial q_1 \partial T}\cdot\frac{\partial q_1}{\partial F_z} = \frac{\partial^2 W}{\partial q_1 \partial T}.
\end{aligned} \tag{A–2}$$

Therefore using (A–1), (A–2) and (8), (14) is obtained.

Appendix B: Largest influence sixty degrees crack orientation

It is noticeable that the variation in the system response is due to the elements of the flexibility matrix. Therefore, any change in the system response is directly related to the flexibility matrix elements. In the following, we will show that, for instance, the maximum value of $c(3,4)$ will happen in an angle of approximately 60 degrees.

Let us consider the following figure:

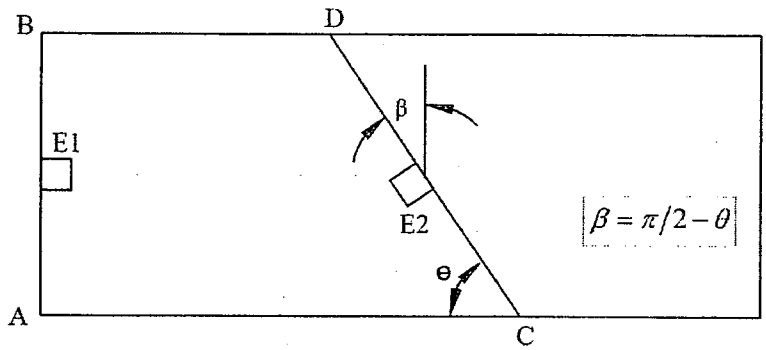

Fig. A–1. E1 and E2 elements for using in Mohr circle

According to this figure, it is evident that if element E1 is just under an axial load, the element E2 with $\beta = \theta = \pi/4$ will experience the maximum shear stress. Also, if the element E1 is under pure shear, the element E2 with $\beta = \theta = \pi/4$ is under axial stress only. However, for cases in which the element is under mixed loads, the maximum shear stress will not happen at an angle of 45 degrees.

Assume that element E1 is under pure shear stress. According to Fig. A–2, the tension and shear stresses for an element after rotation of β in CCW direction, is expressed as:

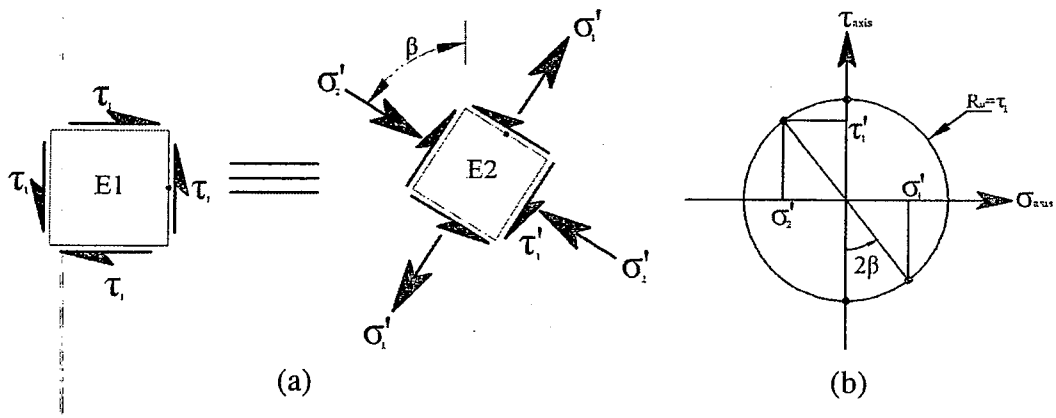

Fig. A–2. a) E1 element and E2 element after β rotation (CCW), b) Mohr circle with center σ_M and radius R_M

$$\sigma_1' = \tau_1 \sin(2\beta) = \tau_1 \sin(\pi - 2\theta) = \tau_1 \sin(2\theta), \tag{A–3}$$

$$\tau_1' = \tau_1 \cos(2\beta) = -\tau_1 \cos(2\theta). \tag{A–4}$$

In the above equations,

$$\tau_1 = \frac{TR}{(\pi R^4/2)} = \frac{2T}{\pi R^3}. \tag{A–5}$$

In a similar way, consider the element E1 which is under uniaxial tension only.

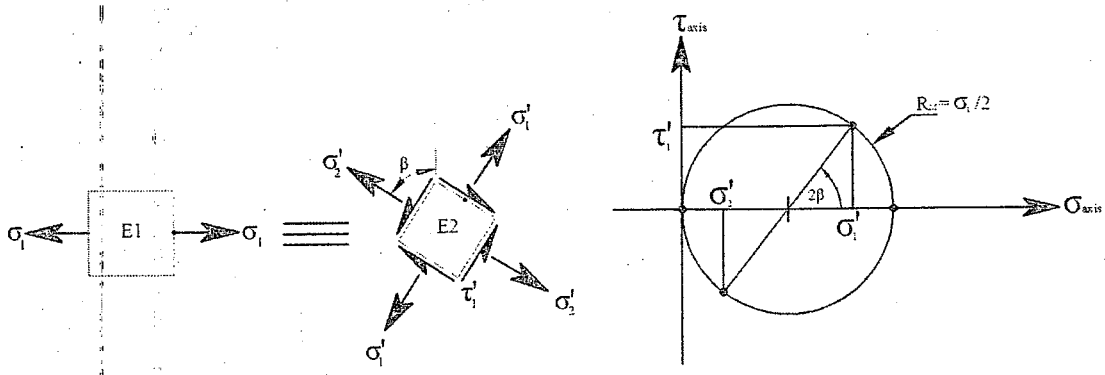

Fig. A–3. a) E1 element and E2 element after β rotation (CCW), b) Mohr circle with center σ_M and radius R_M

The shear and axial stresses for a rotated element with angle β in CCW direction can be expressed as:

$$\sigma_1' = \frac{\sigma_1}{2} + \frac{\sigma_1}{2}\cos(2\beta) = \frac{\sigma_1}{2}(1+\cos(\pi - 2\theta)) = \sigma_1 \sin^2(\theta), \tag{A–6}$$

$$\tau_1' = \frac{\sigma_1}{2}\cos(2\beta) = \frac{\sigma_1}{2}\sin(2\theta) = \sigma_1 \sin(\theta)\cos(\theta). \tag{A–7}$$

In the above equations σ_1 is:

$$\sigma_1 = \frac{q_1}{\pi R^2}. \tag{A–8}$$

Therefore, the maximum tension and shear stresses for an element under combined loading is:

$$\sigma_{\max} = \frac{2T}{\pi R^3}\sin(2\theta) + \frac{q_1}{\pi R^2}\sin^2(\theta), \tag{A–9}$$

$$\tau_{\max} = -\frac{2T}{\pi R^3}\cos(2\theta) + \frac{q_1}{\pi R^2}\sin(\theta)\cos(\theta). \tag{A–10}$$

According to Eqs. (21) and (22) in calculating the elements of flexibility matrix, the squared of $\sigma_{\max}$ and $\tau_{\max}$ need to be calculated:

$$\sigma_{\max}^2 = \left(\frac{q_1}{\pi R^2}\sin^2(\theta) + \frac{2T}{\pi R^3}\sin(2\theta) + \ldots\right)^2, \tag{A–11}$$

$$\tau_{\max}^2 = \left(-\frac{2T}{\pi R^3}\cos(2\theta) + \frac{q_1}{\pi R^2}\sin(\theta)\cos(\theta) + \ldots\right)^2. \tag{A–12}$$

To determine the element $c(3,4)$, one should compute the second derivatives of of $\sigma_{\max}^2$ and $\tau_{\max}^2$ with respect to q_1 and T

$$\frac{\partial^2 \sigma_{\max}^2}{\partial q_1 \partial T} = \frac{\partial^2}{\partial q_1 \partial T}\left(\frac{q_1}{\pi R^2}\sin^2(\theta) + \frac{2T}{\pi R^3}\sin(2\theta) + \ldots\right)^2 = 2\left(\frac{2}{\pi R^3}\right)\left(\frac{1}{\pi R^2}\right)\sin^2(\theta)\sin(2\theta), \tag{A–13}$$

$$\frac{\partial^2 \tau_{\max}^2}{\partial q_1 \partial T} = \frac{\partial^2}{\partial q_1 \partial T}\left(-\frac{2T}{\pi R^3}\cos(2\theta) + \frac{q_1}{\pi R^2}\sin(\theta)\cos(\theta) + \ldots\right)^2 = -2\left(\frac{2}{\pi R^3}\right)\left(\frac{1}{\pi R^2}\right)\sin(\theta)\cos(\theta)\cos(2\theta). \tag{A–14}$$

Therefore, the element $c(3,4)$ of the flexibility matrix is proportional to function H in the following equation:

$$H(\theta) = \frac{\partial^2 \sigma_{\max}^2}{\partial q_1 \partial T} + \frac{\partial^2 \tau_{\max}^2}{\partial q_1 \partial T} = 2\left(\frac{2}{\pi R^3}\right)\left(\frac{1}{\pi R^2}\right) F(\theta), \quad \text{(A–15)}$$

$$F(\theta) = \sin^2(\theta)\sin(2\theta) - \sin(\theta)\cos(\theta)\cos(2\theta). \quad \text{(A–16)}$$

The variation of $F(\theta)$ as a function of θ is shown in the following figure. The plot shows that the maximum occurs in an angle of 60 approximately.

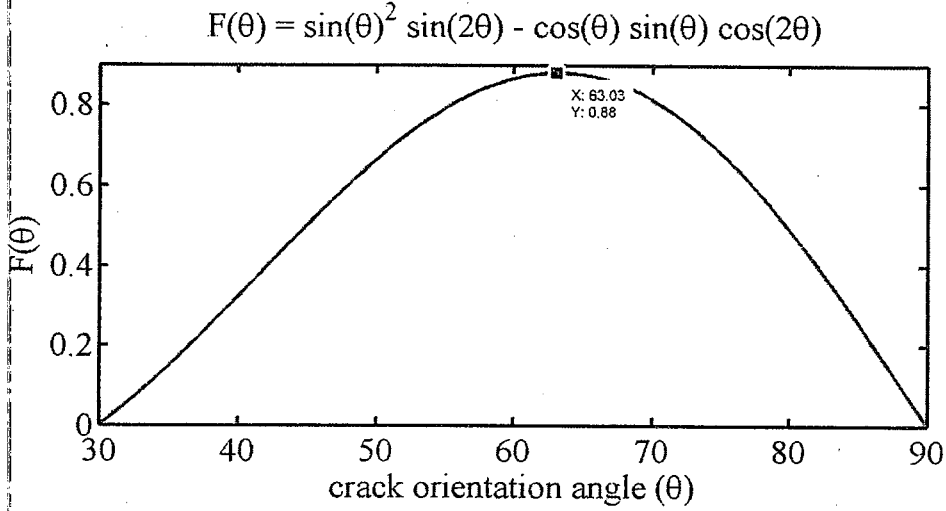

Fig. A–4. The variation of $F(\theta)$ versus of θ

References

[1] Darpe, A. K., Dynamics of a Jeffcott rotor with slant crack, Journal of Sound and Vibration 303 (2007) 1–28.

[2] Darpe, A. K., Gupta, K., Chawla, A., Coupled bending, longitudinal and torsional vibrations of a cracked rotor, Journal of Sound and Vibration 269 (2004) 33–60.

[3] Darpe, A. K., Gupta, K., Chawla, A., Dynamics of a two cracked rotor, Journal of Sound and Vibration 259 (3) (2003) 649–675.

[4] Darpe, A. K., Gupta, K., Chawla, A., Transient response and breathing behaviour of a cracked Jeffcott rotor, Journal of Sound and Vibration 272 (2004) 207–243.

[5] Ichimonji, M., Watanabe, S., The dynamics of a rotor system with a shaft having a slant crack, JSME, International Journal, Series III 31 (4) (1988) 712–718.

[6] Ichimonji, M., Kazao, S., Watanabe, S., Nonaka, S., The dynamics of a rotor system with a slant crack under torsional vibration, Nonlinear and Stochastic Dynamics 78 (1994) 81–89.

[7] Lin, Y., Chu, F., The dynamic behaviour of a rotor system with a slant crack on the shaft, Mechanical System and Signal Processing 24 (2010) 522–545.

[8] Papadopoulos, C. A., The strain energy release approach for modeling cracks in rotors: a state of the art review, Mechanical Systems and Signal Processing 22 (2008) 763–789.

[9] Papadopoulos, C. A., Dimarogonas, A. D., Stability of cracked rotors in the coupled vibration mode, Journal of Vibration Acoustics Stress and Reliability in Design-Transactions of the ASME 110 (3) (1988) 356–359.

[10] Sekhar, A. S., Mohanty, A. R., Prabhakar, S., Vibrations of cracked rotor system: transverse crack versus slant crack, Journal of Sound and Vibration 279 (2005) 1 203–1 217.

[11] Tada, H., Paris, P. C., Irwin, G. R., The stress analysis of cracks, Handbook, third edition, Professional Engineering Publishing, 2000.